Food Research International 66 (2014) 140–149

Contents lists available at ScienceDirect

Food Research International

journal homepage: www.elsevier.com/locate/foodres

The properties of whey protein–carrageenan mixtures during the formation of electrostatic coupled biopolymer and emulsion gels

Ricky S.H. Lam, Michael T. Nickerson *

Department of Food and Bioproduct Sciences, University of Saskatchewan, 51 Campus Drive, Saskatoon, SK S7N 5A8, Canada

ARTICLE INFO

Article history:
Received 15 April 2014
Accepted 14 August 2014
Available online 21 August 2014

Keywords:
Whey protein
Carrageenan
Coacervates
Emulsion gels

ABSTRACT

The rheological properties of whey protein isolate (WPI) and WPI with carrageenan (CG) (kappa-, iota- and lambda-types) mixtures during a slow acidification process were investigated in a non-emulsified and emulsified system. For all systems, electrostatically coupled networks were formed leading to the formation of a biopolymer or emulsion-based gel network. However, network strength differed depending on the CG-type. In the case of biopolymer gels, the storage modulus within the plateau zone for WPI–kappa-CG and WPI–iota-CG mixtures were ~93 and ~73 Pa, respectively, whereas the WPI–lambda-CG network was weaker (~8 Pa). The gel point corresponded to the pH where complex coacervation occurred. WPI–CG mixtures were also able to lower interfacial tension from 28 to 18–22 mN/m before gelation. Emulsion gels followed a similar trend as the biopolymer networks, except they were stronger (WPI–kappa-CG, WPI–iota-CG and WPI–lambda-CG systems had storage moduli of ~435, ~320 Pa and ~103 Pa, respectively). The presence of CG decreased the average droplet size of these emulsions from ~38 to ~ 32 μm, regardless of the CG type. Protein stabilized emulsion gels were presumed to form, where upon complexation with CG, flocculation between droplets was promoted until an electrostatic-stabilized gel network was formed within the continuous phase. The WPI control did not gel for both non-emulsified and emulsified systems.

1. Introduction

Proteins and polysaccharides are common ingredients in many food systems because of their gelling, thickening and/or emulsifying properties. However, they often require tailoring of their physicochemical properties to control precipitation and aggregation which influences their rheological or emulsion forming/stabilizing properties. In combination, proteins and polysaccharides have been reported to form electrostatic complexes *via* attractive forces under suitable pH and solvent conditions where biopolymers have opposing net charges (Turgeon, Schmitt, & Sanchez, 2007). The coacervation process (also known as associative phase separation) has been well studied and reviewed in the literature (de Kruif, Weinbreck, & de Vries, 2004; Dickinson, 2008; Turgeon et al., 2007). The process involves separation of electrostatically attracted proteins and polysaccharides into a biopolymer-rich lower phase, and the formation of an upper solvent-rich phase within an aqueous mixture (Weinbreck, de Vries, Schrooyen, & de Kruif, 2003). During a pH-induced coacervation, proteins and negatively charged polysaccharides initially interact near the protein's isoelectric point below which it assumes a net positive charge. The point of initial interactions as event by a slight change in optical density is known as pH_c, signifying the formation of 'soluble complexes' (de Kruif et al., 2004). As pH decreases further, macroscopic phase separation occurs and a large rise in optical density initiates at a pH, noted as $pH_{\phi 1}$ signifying the formation of 'insoluble complexes' (de Kruif et al., 2004). The terms: 'soluble and insoluble', are used to describe the level of biopolymer interactions rather than specific functionality testing (de Kruif et al., 2004). Biopolymer interactions reach a maximum at pH_{opt} associated with a maximum optical density and where the overall charge of the biopolymers is close to zero (de Kruif et al., 2004). And then complexes undergo dissolution as pH approaches the pK_a of the reactive sites on the polysaccharide, denoted as $pH_{\phi 2}$. Depending on the strength of biopolymer interactions, coacervate or precipitate structures may form. The coacervate structure is able to entrap a lot of solvent which allows it to remain suspended and have high biopolymer mobility (de Kruif et al., 2004), and typically occurs involving both a strong and weakly charged biopolymer, such as WPI and gum arabic, respectively (Weinbreck et al., 2003). In contrast, precipitate-type structures tend to fall out of solution quickly, and have significantly less entrapped solvent and biopolymer mobility (de Kruif et al., 2004), and typically involve two strongly charged biopolymers (*e.g.*, WPI and carrageenan (CG)) (Weinbreck, Nieuwenhuijse, Robjijn, & de Kruif, 2004).

Although coacervation studies are not limiting in the literature, systems shown to form electrostatic coupled biopolymer and emulsion networks are few. For instance, Singh, Aswal, and Bohidar (2007) reported electrostatic coupled networks to form in mixtures of agar–gelatin, Yuan, Wang, Yang, and Yin (2014) with soy protein–chitosan

* Corresponding author. Tel.: +1 306 966 5030; fax: +1 306 966 8898.
E-mail address: Michael.Nickerson@usask.ca (M.T. Nickerson).

http://dx.doi.org/10.1016/j.foodres.2014.08.006
0963-9969/

and Schmidt, Cousin, Huchon, Boue, and Axelos (2009) with lysozyme–pectin. In the present study the formation of electrostatic coupled biopolymer and emulsion gels using WPI and CG mixtures, as a function of CG-type were studied. Whey proteins (α-lactalbumin and β-lactoglobulin) from bovine milk have been extensively studied for their emulsifying (Britten & Giroux, 1991; Hu, McClements, & Decker, 2004; Reiffers-Magnani, Cuq, & Watzke, 2000), gelling (Elofsson, Dejmek, Paulsson, & Burling, 1997; Gulzar, Lechevalier, Bouhallab, & Croguennec, 2012; Tang, McCarthy, & Munro, 1994) and surface active properties (Davis & Foegeding, 2007; Patino, Nino, & Sanchez, 1999; Yang & Foegeding, 2011). CG is a family of anionic polysaccharide extracted from red seaweed (*Rhodophyta* species), commonly used as a gelling or thickening agent by the food industry (Campo, Kawano, de Silva, & Carvalho, 2009; Trius, Sebranek, & Lanier, 1996; van de Velde, Knutsen, Usov, Rollema, & Cerezo, 2002). Their physicochemical properties have also been very well characterized (Piculell, Nilsson, & Muhrbeck, 1992; Souza, Hilliou, Bastos, & Goncalves, 2011; Thanh et al., 2002) and reviewed (Campo et al., 2009; Rinaudo, 2006). CGs are typically comprised of a disaccharide repeating unit comprised of D-galactose and 3,6-anhydro-D-galactose residues which are sulfated with 1, 2 or 3 groups per disaccharide repeating unit which corresponds to κ-, ι- and λ-type CG, respectively (Campo et al., 2009; Weinbreck et al., 2004). In addition to these three types, three others have also been identified (μ-, ν- and θ-types) by Knutsen, Myladobodski, Larsen, and Usov (1994) however these are more minor in comparison. The use of CG of varying types allows for the effect of linear charge density on biopolymer interactions and their ability to alter the rheological properties.

Complex coacervates have been previously reported to improve on emulsion stability (Koupantsis, Pavlidou, & Paraskevopoulou, 2014; Li & McClements, 2011; Nakagawa, Iwamoto, Nakajima, Shono, & Satoh, 2004). In some cases, emulsions may take on a gel-like nature (Dickinson, 2012). In the food industry, these protein-based gels containing emulsions are typically found as yoghurts, cheeses, sauces and reformulated meat products (sausages, patés, *etc.*) (Dickinson, 2012). Typically, emulsion gels are characterized into two main categories: emulsion-filled protein gels and protein-stabilized emulsion gels (Dickinson, 2012). The primary difference between these two types of emulsion gels are their internal structure. In emulsion-filled protein gels, the continuous aqueous phase is gelled with oil droplets dispersed within this gelled biopolymer network (Dickinson, 2012). In protein-stabilized emulsion gels, structure is attributed to the inter-connected flocculated network of oil droplets stabilized by the interfacial biopolymer film (Dickinson, 2012). Stone & Nickerson (2012) investigated the formation of electrostatic complexes involving WPI and CG molecules as a function of CG type under dilute conditions (0.25% w/w), and then their emulsion stabilizing effects at a 1.0% (w/w) total biopolymer concentration with a 1:1 biopolymer solution to oil ratio. The authors reported this ratio to occur at 12:1 for WPI–κ-CG and WPI–λ-CG mixtures, and 20:1 for the WPI–ι-CG system (Stone & Nickerson, 2012). Maximum complexation of all mixtures was found to occur near pH 4.50. Furthermore, the authors reported that the WPI–CG mixtures regardless of the CG –type enhanced the emulsion stability over WPI alone, but did not explore the underlining mechanisms.

The overall goal of the present study is to examine the underlining mechanisms driving the formation of WPI–CG coupled biopolymer and emulsion gel networks, as a function of CG-type. This information is essential for controlling and optimizing their use in food or controlled delivery-type applications.

2. Materials and methods

2.1. Materials

WPI used in this study was generously donated by Davidson Foods International, Inc. (Le Sueur, MN, USA). The chemical composition of the commercial WPI powder was determined according to AOAC (2003) methods; 925.10 (moisture), 923.03 (ash), 920.87 (crude protein), and 920.85 (lipid). Carbohydrate content was determined on the basis of present differential from 100%. The WPI powder comprised of 89.78% protein (%N × 6.38), 0.10% lipid, 4.92% moisture, 2.06% ash (including 0.08% Ca^{2+}, 0.01% Mg^{2+}, 0.02% K^{+}, and 0.66% Na^{+}), and 3.13% carbohydrate (wet basis). CG (κ-, ι-, and λ-) and glucono-δ-lactone (GDL) were purchased from Sigma-Aldrich (Oakville, ON, Canada). For all three types of CG, the supplier provided their compositional information where κ-CG was comprised of 66.50% carbohydrate, 10.65% moisture and 22.86% ash (including 2.4% Ca^{2+}, 0.16% Mg^{2+}, 5.4% K^{+}, 0.49% Na^{+}); ι-CG contained 64.40% carbohydrate, 10.82% moisture and 24.97% ash (including 3.4% Ca^{2+}, 0.18% Mg^{2+}, 3.2% K^{+}, 1.2% Na^{+}); and λ-CG contained 63.79% carbohydrate, 12.26% moisture and 23.95% ash (including 3.0% Ca^{2+}, 0.83% Mg^{2+}, 2.4% K^{+}, 1.3% Na^{+}). For κ-, ι-, and λ-CG, their molecular weights were ~154 kDa, ~250 kDa and ~250 kDa respectively. Canola oil used in this study was purchased from a local supermarket. All other chemicals used in this study were of reagent grade and purchased through Sigma-Aldrich (Oakville, ON, Canada). The water used for all biopolymer mixtures was filtered using a Millipore Milli-Q™ water purification system (Millipore Corp., Milford, MA, USA). The WPI protein and CG solutions were corrected for protein and carbohydrate contents respectively and used without further purification.

2.2. Sample preparation

Biopolymer solutions (1.0% w/w biopolymer) were prepared by dispersing WPI and CG (κ-, ι-, and λ-type) in water by mechanical stirring (500 rpm) at room temperature (21–23 °C) for 60 min. A homogenous WPI solution (1.0% w/w) was also prepared as a control. A mixing ratio for WPI with κ-, ι- and λ-CG solutions of 12:1, 20:1 and 12:1, respectively was chosen based on work by Stone & Nickerson (2012), and correspond to the optimal complexation ratio. After 60 min of mixing, 0.5% w/w GDL was added to the biopolymer solution and then stirred for 1 min just prior to analysis to slowly start acidifying the solution. Changes in pH were measured using a pH meter (Thermo Scientific, Madison, WI, USA) from pH ~7.00 to ~4.20 within all three mixtures and an individual WPI solution and plotted vs. time.

Oil-in-water emulsions were prepared by first preparing the biopolymer solution as described above, followed by the addition of oil immediately after the addition of GDL at an oil:water ratio of 1:1 to a total weight of 10 g. This biopolymer–oil mixture was then homogenized at 7200 rpm for 5 min using an Omni Macro Homogenizer (Omni International Inc., Marietta, GA) equipped with a 20 mm saw tooth generating probe.

2.3. Turbidimetric pH-titration over time for WPI:carrageenan mixtures

The optical density (OD) for WPI:carrageenan mixtures at a concentration of 1.0% (w/w) were assessed over time during the slow acidification by GDL using a UV–vis spectrophotometer (Thermo Scientific, Madison, WI) at 600 nm. Plastic cuvettes with a 1 cm path length were used. Measurements were taken every 1 min for a total of 90 min. A 1.0% (w/w) WPI solution was also measured as a control. The critical pH associated with the formation of insoluble complexes was also evident at a pH (denoted as $pH_{\phi 1}$) corresponding to where macroscopic phase separation occurs corresponding to large increases in OD. This critical pH value was determined by extending the tangent of the steepest part of the rise to the OD baseline. Each critical pH was determined for individual curves, and then reported as the mean ± one standard deviation ($n = 3$).

2.4. Interfacial tension

The interfacial tension for each WPI:carrageenan mixture (1.0% w/w) and the WPI control was measured using a Lauda TD 2 Tensiometer

(Lauda-Königshofen, Germany) equipped with a Du Nüoy ring (20 mm diameter). Within a 40 mm diameter glass sample cup, a 20 mL biopolymer solution was added then stirred for 1 min after the addition of 0.5% (w/w) GDL, followed by the immersion of the Du Noüy ring and then the addition of an upper canola oil layer (20 mL). The ring was then pulled upward to stretch the interface to measure the maximum force without breaking into the oil phase. Interfacial tension measurements (mN/m) were taken every 600 s where the mean of three replicates ± one standard deviation is presented at each data point. Interfacial tension was calculated from the maximum force (F_{max}; units: milli-Newton; instrument measures force as mg × gravity) using the following equation (Eq. (1)):

$$\gamma = \frac{F_{max}}{4\pi R\beta} \quad (1)$$

where, γ is the interfacial tension (mN/m), R is the radius of the ring (20 mm), and β is a correction factor that depends on the dimensions of the ring and the density of the liquid involved (McClements, 2005).

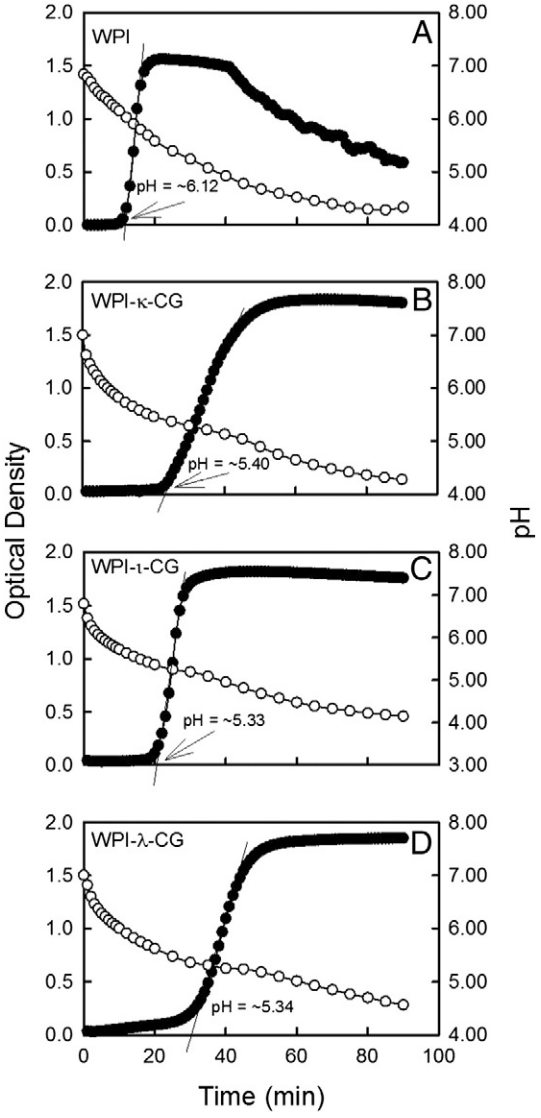

Fig. 1. Changes to the optical density for an individual WPI (A) solution and mixtures of WPI and κ-CG (B), ι-CG (C) and λ-CG (D) solutions as a function of pH (open circles) and time (min). Curves represent the mean optical density for 3 separate samples. All solutions had a total biopolymer concentration of 1.0 % (w/w) and were acidified using 0.5% (w/w) GDL.

All measurements are reported as the mean ± one standard deviation (n = 3).

2.5. Small deformation rheology

Small deformation rheology was used to measure changes to the biopolymer and emulsion solutions during acidification by GDL (*i.e.*, WPI:carrageenan; WPI control). Approximately 1.5 mL of the biopolymer or emulsion solution with GDL was placed onto a AR-G2 Rheometer (TA Instruments, New Castle, DE) equipped with a 40 mm diameter 2° acrylic cone. A time sweep was conducted to capture the gelation process for 90 min where measurements were made at 1 Hz every 10 s, where the maximum amplitude for strain was set at 1.0%. Following a time sweep, frequency and strain sweeps were measured. Frequency sweeps were used to characterize the gel formed where the maximum strain was set to 1.0% with frequencies ranging from 0.05 Hz to 100 Hz while capturing 15 points per logarithmic decade. Strain sweeps were used to characterize the physical properties of the gel where strains of 0.01% to 500% with 15 data points per logarithmic decade captured at 5 Hz was also taken. All measurements were made within the linear viscoelastic regime and in triplicates.

2.6. Light microscopy

A Nikon Eclipse E400 light microscope equipped with a Nikon DS-FiL color camera and a long working distance 10× lens and condenser (Nikon Instruments Inc., Melville, NY, USA) was used to capture brightfield micrographs. Images of a drop of the prepared emulsion

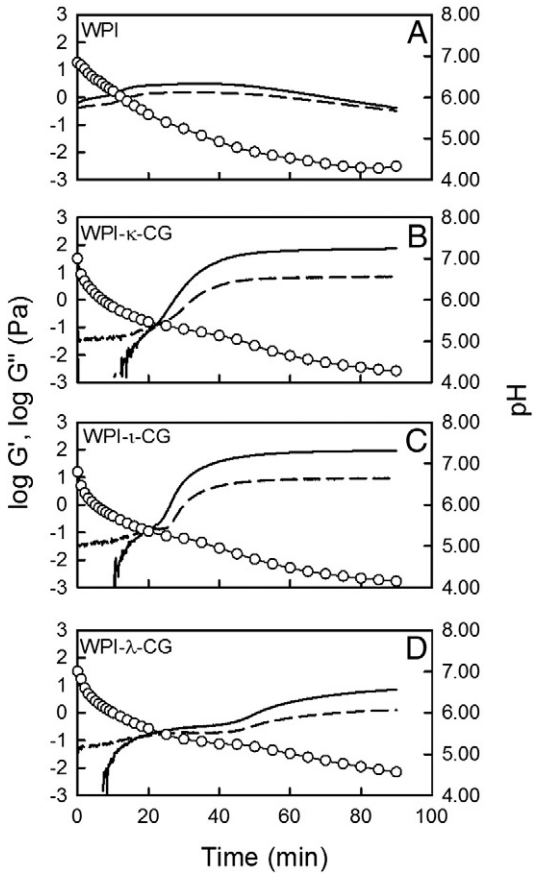

Fig. 2. Dynamic viscoelastic storage (G' (solid line)) and loss (G″ (dashed line)) moduli at 1.0% strain and at a frequency of 1 Hz for an individual WPI (A) solution and mixtures of WPI and κ-CG (B), ι-CG (C) and λ-CG (D) as a function of pH (open circles) and time (min). Each curve is representative of 3 separate time sweep runs on separate samples. All solutions had a total biopolymer concentration of 1.0% (w/w) and were acidified using 0.5% (w/w) GDL.

with a coverslip after a 90 min time period at 10× magnification (pH = ~4.20) were captured. Images were captured at a resolution of 2560 by 1920 pixels and analyzed using ImageJ (National Institutes of Health, Bethesda, MD, USA) to determine the width of emulsion droplets. Fifty droplets were measured and averaged per slide and the average of three slides ± one standard deviation was reported for each sample.

2.7. Statistics

The critical pH associated with the formation of insoluble complexes was determined from the turbidity curves and analyzed for statistical significance. Experiments were collected in triplicate for all WPI–CG types and the control WPI solution. A one-way analysis of variance (ANOVA) with Tukey's post hoc analysis was conducted to test for significance among the various WPI–CG types and WPI alone. Statistical analysis was performed with Systat (SPSS Inc., Ver. 10, 2000, Chicago, IL).

3. Results and discussion

3.1. Turbidimetric pH titrations

Optical density (OD) for an individual WPI solution and mixture of WPI and κ-CG (B), ι-CG (C) and λ-CG during a slow acidification process using GDL over time is given in Fig. 1. In the case of the WPI control (Fig. 1A), a rise in OD initially occurred at pH 6.15 ± 0.32 (~7 min), then peaked at an OD of 1.56 at pH 5.58 ± 0.18 (~20 min), followed by a steady decline to an OD of 0.60 at pH 4.33 ± 0.02 (90 min) where the pH became stable. The rise and decline in OD are believed to be associated with protein–protein aggregation near the protein's isoelectric point (pI = 4.6 (Parris & Baginski, 1991)) where it assumes no net charge in solution. The larger aggregates are more effective at scattering light, leading to the change in OD.

Net neutrality of a WPI solution at 25 °C was found to occur near 5.1 (data not shown), suggesting that interactions in the present study are initiated when both WPI and CG molecules are carrying a net negative charge. It is presumed that at these pHs, the highly charged CG is electrostatically binding *via* attractive forces to positively charged patches on the protein's surface and charge fluctuations on the protein's surface near its pI (Stone & Nickerson, 2012; Weinbreck et al., 2004). Others have reported a similar phenomenon for protein–polysaccharides interacting under net negative conditions in mixtures of proteins with highly charged polyelectrolytes, such as bovine serum albumin–acacia gum (Dubin, Gao, & Mattison, 1994), whey proteins–gum arabic (Weinbreck et al., 2003), and gelatin–agar (Boral & Bohidar, 2010).

The addition of CG, regardless of the type, resulted in a shift towards more acidic pHs in the pH associated with the start of the large rise in OD with pH (Fig. 1, B–D). Within complex coacervation literature, this

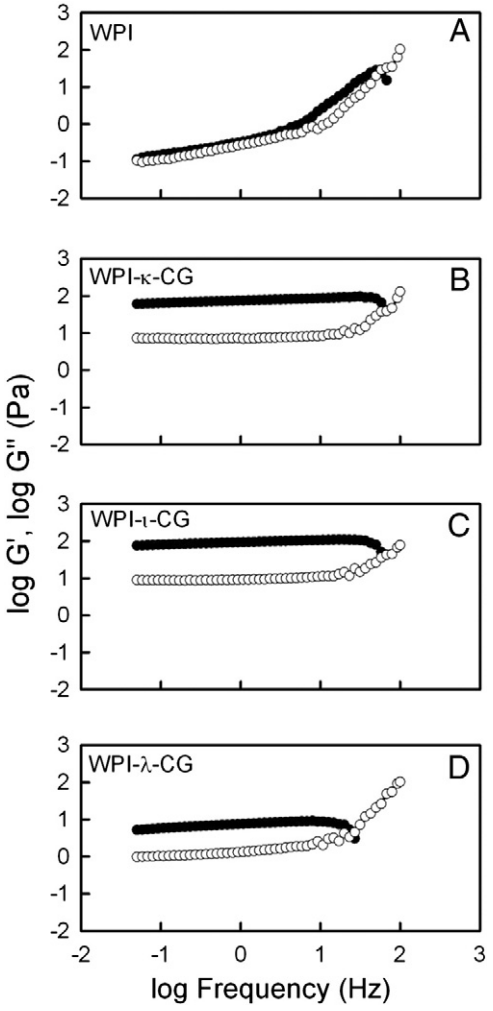

Fig. 3. Dynamic viscoelastic storage (G' (solid circles)) and loss (G″ (open circles)) moduli for an individual WPI (A) solution and mixtures of WPI and κ-CG (B), ι-CG (C) and λ-CG (D) as a function of frequency (Hz) (on double logarithmic axes) with 1.0% strain after 90 min of acidification with 0.5% (w/w) GDL and, after running the time sweep measurements.. All solutions had a total biopolymer concentration of 1.0% (w/w) and were at a pH of ~4.0-4.3 when measured.

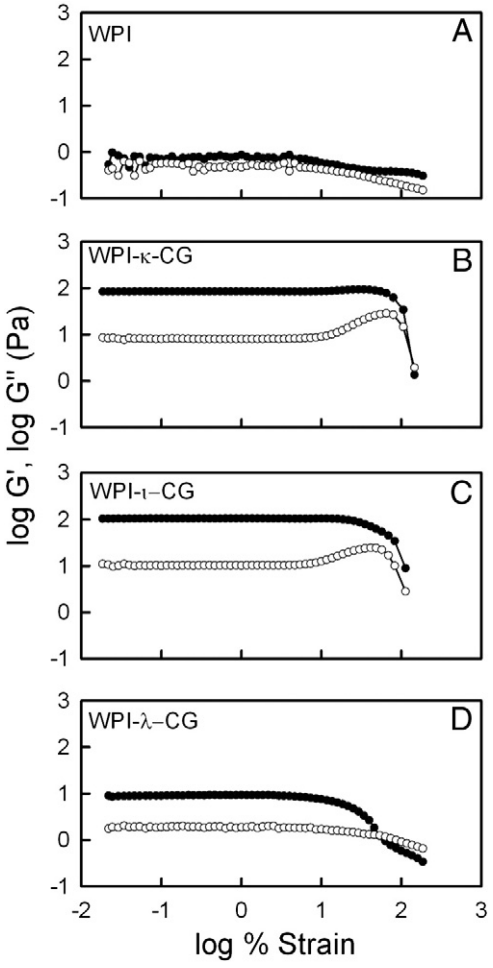

Fig. 4. Dynamic viscoelastic storage (G' (solid circles)) and loss (G″ (open circles)) moduli for an individual WPI (A) solution and mixtures of WPI and κ-CG (B), ι-CG (C) and λ-CG (D) as a function of shear strain (%) (on double logarithmic axes) at a frequency of 1 Hz after 90 min of acidification with 0.5% (w/w) GDL and, after running both the time and frequency sweep measurements. All solutions had a total biopolymer concentration of 1.0% (w/w) and were at a pH of ~4.0-4.3 when measured.

critical pH is known as $pH_{\phi 1}$ which refers to where macroscopic phase separation occurs associated with the formation of insoluble complexes due to the electrostatic attraction of anionic carrageenan molecules and the whey proteins. The initial suppression of OD at higher pH is presumed to be the result of electrostatic repulsion between neighboring CG molecules which inhibited WPI–WPI aggregation. A shift in $pH_{\phi 1}$ from pH 6.12 (WPI control) to 5.40, 5.33 and 5.34 was observed with the addition of κ-CG. ι-CG and λ-CG, respectively (Fig. 1). A one-way ANOVA with Tukey's post hoc analysis revealed a significant difference ($p < 0.001$) for WPI control compared to samples with CG while there was no significant difference between samples with CG. The shift in pH is believed to be associated with the linear charge density of the various types of CG in solution. For instance, κ-, ι- and λ-type CGs have 1, 2 and 3 sulfate reactive sites per disaccharide repeating unit on the polysaccharide backbone, respectively (Campo et al., 2009; Weinbreck et al., 2004), however the ordered conformation of the various types in solution differs. In the literature, the ordered conformation for the κ- and ι-types is thought to be a double helical structure (Rees, Scott, & Williamson, 1970), aggregated single helices (Grasdalen & Smidsrød, 1981) or aggregated helical dimers (Rochas & Landry, 1987), whereas the λ-type lacks an ordered conformation and behaves as a random coil due to the presence of a large number of sulfate groups that inhibits folding (Rochas, Rinaudo, & Vincendon, 1980). Assuming in the present study that the ordered conformations exist for both κ- and ι-types, then the larger shift would be explained by the higher linear charge density of the ι-type CG chain. In contrast, the λ-type follows a different trend since it lacks an ordered conformation in solution. A similar linear charge/conformation dependence of CG was proposed by Stone & Nickerson (2012) to described differences in magnitude for the maximum OD values; however the authors did not report the same trend with $pH_{\phi 1}$ as in the present study. The differences were attributed to the method of acidification (GDL in the present study versus HCl used by Stone & Nickerson (2012)) and their rate of acidification which would have been greater in the present study.

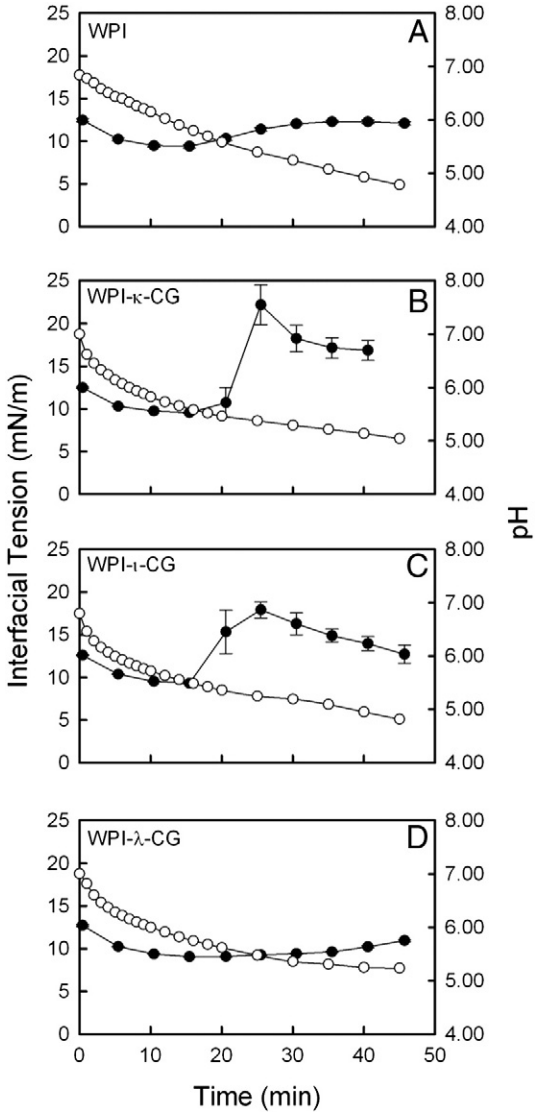

Fig. 5. Interfacial tension (nM/m) (solid circle) and pH (open circle) for an individual WPI (A) solution and mixtures of WPI and κ-CG (B), ι-CG (C) and λ-CG (D) as a function of time (min). Interfacial data represent the mean values ± one standard deviation. All solutions had a total biopolymer concentration of 1.0% (w/w) and were acidified using 0.5% (w/w) GDL.

3.2. Rheology of WPI and WPI–carrageenan solutions

The dynamic storage (*i.e.*, elastic component) and loss (*i.e.*, viscous component) of an individual WPI solution and WPI–CG mixtures were investigated at a constant frequency as a function of time and pH during GDL acidification (Fig. 2). In the case of WPI, no gel networks were formed despite having a slightly higher storage modulus (G′) than loss modulus (G″) (Fig. 2A). The higher elastic component is attributed to the formation of WPI–WPI aggregates which was further confirmed by frequency dependence of this solution under a frequency sweep.

However, as CG is added and pH is reduced, complexation with the WPI molecules leads to substantial changes to the viscoelastic spectrum. Based on the aforementioned OD data, $pH_{\phi 1}$ for WPI–κ-CG, WPI–ι-CG and WPI–λ-CG mixtures occurred at 5.34, 5.33 and 5.40, respectively

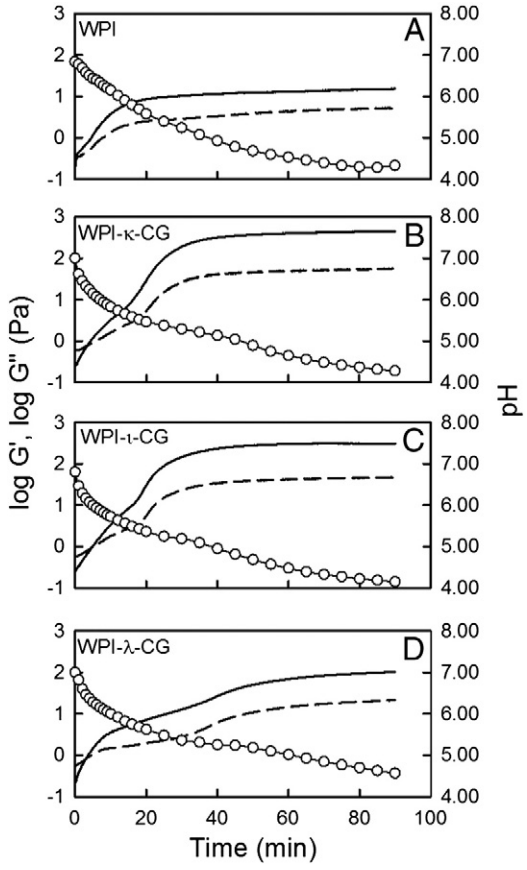

Fig. 6. Dynamic viscoelastic storage (G' (solid line)) and loss (G″ (dashed line)) moduli at 1.0% strain and at a frequency of 1 Hz for emulsions stabilized by an individual WPI (A) solution and mixtures of WPI and κ-CG (B), ι-CG (C) and λ-CG (D) as a function of pH (open circles) and time (min). Each curve is representative of 3 separate time sweep runs on separate samples. All solutions had a total biopolymer concentration of 1.0% (w/w) and were acidified using 0.5% (w/w)GDL.

(Fig. 1B–D). For these systems, G′ < G″ at pHs > ~5.33 for WPI–κ-CG and WPI–ι-CG; and pHs > ~5.53 for WPI–λ-CG mixtures indicating that the biopolymer mixtures were within the flow region of the viscoelastic spectrum behaving as a liquid (Fig. 2B–D). The magnitude of G′ of these WPI–CG mixtures was also lower than that of WPI over this time (and pH region) indicating that the material was less structured likely due to electrostatic repulsion between neighboring CG molecules. However, at pHs < ~5.33 for WPI–κ-CG and WPI–ι-CG, G′ became greater than G″ (denoted as the gel point), after which a gel network was formed in the case of WPI–κ-CG and WPI–ι-CG mixtures (Fig. 2B, C). In this case, both viscoelastic moduli increased up to a plateau after ~40 min (or ~pH 5.00). In contrast, greater time/pH dependence of the viscoelastic data, and reduced magnitude of G′ was observed for the WPI–λ-CG mixture relative to the WPI–κ-CG and WPI–ι-CG mixtures suggesting that there is most likely a very weak gel network (Fig. 2D). The G′ in the plateau region for WPI–κ-CG and WPI–ι-CG mixtures was ~93 Pa and ~73 Pa, respectively, whereas the G′ of the WPI–λ-CG mixture after 90 min (pH ~4.4) was much weaker at ~8 Pa and never reached a plateau zone. The significantly reduced network strength in the WPI–λ-CG mixture is most likely due to the large number of sulfate groups (3×) per repeating disaccharide units which makes λ-CG on its own a non-gelling polysaccharide. This would inhibit extensive ordering into network junction zones if sulfate groups were left free or unbound to the WPI. In contrast, both κ-CG and ι-CG are known for their gelling abilities and rigid network structures.

Complexation between WPI and CG has been previously reported by Alizadeh-Pasdar, Nakai, and Li-Chan (2002) and Harrington, Foegeding, Mulvihill, and Morris (2009). Alizadeh-Pasdar et al. noted conformational changes to WPI upon complexation with CG, possibly opening itself up for improved gelling abilities. Harrington et al. studied the gelation properties of the mixed biopolymer solutions to find that WPI and CG were capable of forming bi-continuous networks. In contrast, Tavares, Monteiro, Moreno, and Lopes da Silva (2005) reported the formation of an electrostatic coupled network between whey proteins and galactomannans, where network stiffness is dependent upon the polysaccharide concentration. In this study, no networks formed with WPI alone (under the concentrations and solvent conditions examined) which suggests that CG's ability to complex with WPI is essential for network formation. To better understand the type of network formed, frequency and strain sweeps were performed to characterize these gels further.

In the present study, after the 90 min acidification period (solution pH ~4.0–4.3), viscoelastic moduli were followed by both frequency (Fig. 3) and strain (Fig. 4) sweeps. Individual WPI solutions were confirmed to be non-gel like, where both G′ and G″ were of similar in magnitude and highly frequency dependent, ranging from ~0.1 to ~30 Pa (Fig. 3A). In contrast, WPI–κ-CG, WPI–ι-CG and WPI–λ-CG mixtures had both viscoelastic moduli to be relatively independent of frequency

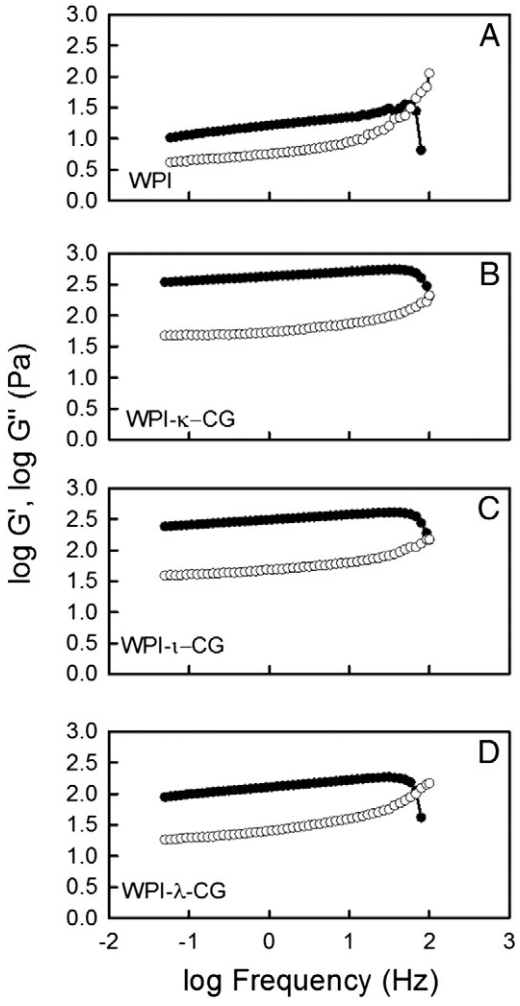

Fig. 7. Dynamic viscoelastic storage (G' (solid circles)) and loss (G″ (open circles)) moduli for emulsions stabilized by an individual WPI (A) solution and mixtures of WPI and κ-CG (B), ι-CG (C) and λ-CG (D) as a function of frequency (Hz) (on double logarithmic axes) with 1.0% strain after 90 min of acidification with 0.5% (w/w) GDL and, after running the time sweep measurements. All solutions had a total biopolymer concentration of 1.0% (w/w) and were at a pH of ~4.0–4.3 when measured.

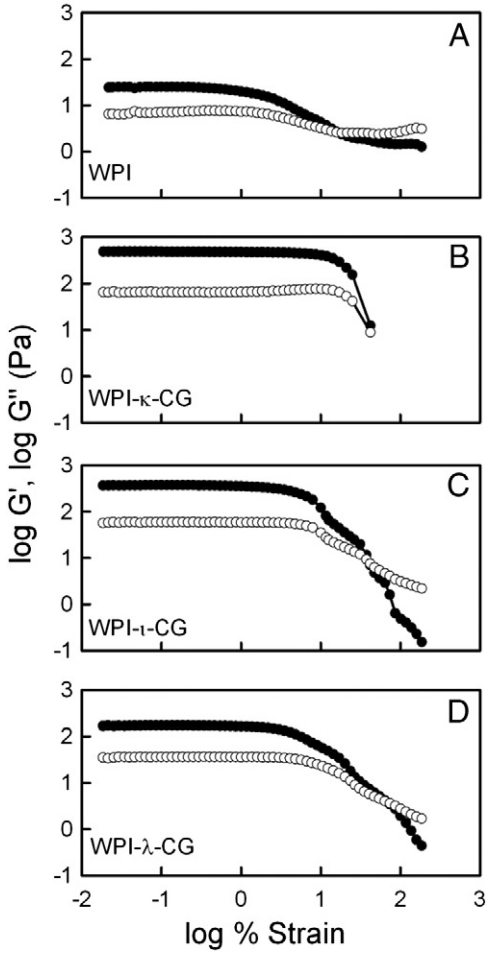

Fig. 8. Dynamic viscoelastic storage (G' (solid circles)) and loss (G″ (open circles)) moduli for emulsions stabilized by an individual WPI (A) solution and mixtures of WPI and κ-CG (B), ι-CG (C) and λ-CG (D) as a function of shear strain (%) (on double logarithmic axes) at a frequency of 1 Hz after 90 min of acidification with 0.5% (w/w) GDL and, after running both the time and frequency sweep measurements. All solutions had a total biopolymer concentration of 1.0% (w/w) and were at a pH of ~4.0–4.3 when measured.

and with G′ > G″, except at higher frequency where we saw an increase in G″ and a corresponding decrease in G′ (Fig. 3B–D). This crossover point in the frequency sweeps where G″ becomes larger than G′ indicates that these are weak gels. In Fig. 3, the crossover point for WPI–λ-CG and WPI–κ-CG occurred at the lowest and highest frequencies respectively indicating that the former was relatively the weakest and the latter being the stronger of the three WPI–CG gels. Similar results were found in the relative strength of collagen hydrogels characterized by frequency sweeps (Hu et al., 2010).

A strain sweep for the WPI solution showed no structure which was expected as this was a solution comprised of WPI aggregates. In contrast, WPI–κ-CG, WPI–ι-CG and WPI–λ-CG mixtures showed a more distinct break in viscoelastic moduli with increasing strain, breaking at ~73.41%, ~74.52% and ~5.38% strains, respectively (Fig. 4). The breakdown of the WPI–κ-CG and WPI–ι-CG networks (as evidenced by G′) was more abrupt with increasing strain than the WPI–λ-CG system, suggesting that they formed stronger network structures. In the case of the WPI–λ-CG system, the more gradual break in G′ reflects the increased polymer mobility within the network allowing for a greater ability to dissipate imposed strain.

3.3. Interfacial properties of WPI and WPI–carrageenan complexes

Interfacial tension measurements for an aqueous system of an individual WPI solution and WPI–CG mixtures were investigated at a water–oil interface as a function of time and pH during a GDL titration (Fig. 5). In general, proteins act to lower the tension at an interface by first migrating towards the interface and then re-aligning to position its hydrophobic moieties towards the oil phase and the hydrophilic moieties towards the aqueous phase; neighboring proteins at the interface then aggregate together to form a viscoelastic film (Tcholakova, Denkov, Ivanov, & Campbell, 2006). Without the presence of any biopolymers, the water–canola oil interface in the present study had an interfacial tension of ~28 mN/m. The addition of WPI caused the interfacial tension to become reduced (~12 mN/m) as the whey proteins became integrated into the interface. For the WPI system, interfacial tension was observed relatively constant over time during GDL acidification ranging between ~10 and ~12 mN/m (Fig. 5A).

In the case of the WPI–κ-CG and WPI–ι-CG systems, interfacial tension was found to be similar to the individual WPI solution during acidification under pH conditions where they were considered to be non-interacting, however abruptly increased at ~pH 5.60 near their $pH_{\phi 1}$ (Fig. 1B,C) and gel point (Fig. 2B,C). The rapid rise in interfacial tension is thought to be associated with the complexation of WPI with the CG chains. The subsequent formation of WPI–κ-CG and WPI–ι-CG gel networks within the aqueous phase near its gel point is hypothesized to offset the equilibrium of proteins at the interface and within the aqueous phase causing previously integrated proteins to be drawn back into the aqueous phase. Interfacial tension was at the highest for WPI–κ-CG and WPI–ι-CG at ~22 (pH 5.37) and ~18 mN/m (pH 5.24), respectively, and then started to decrease again over time/acidification as a new equilibrium tries to become established. Findings suggests that some of the electrostatic complexes may be moving back towards the oil–water interface over time and re-integrating into it. In contrast, the WPI–λ-CG system behaved very similarly to the individual WPI solution most likely since the attractive forces between WPI–λ-CG were too weak to pull the WPI from its equilibrium at the interface to disrupt the interfacial tension. Interfacial tension data was measured only till ~45 min since for both WPI–κ-CG and WPI–ι-CG, further acidification resulted in increased elasticity of the formed electrostatic network,

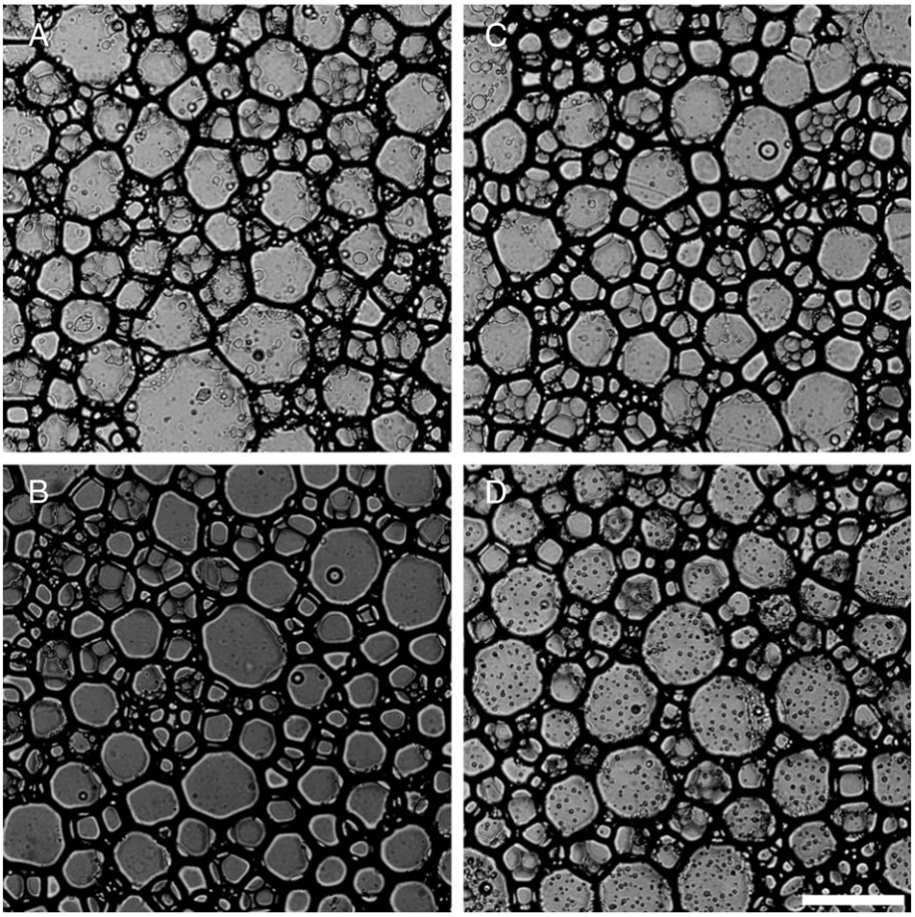

Fig. 9. Brightfield microscopy of emulsion gels stabilized with WPI-κ-CG (A), WPI- ι-CG (B) and WPI-λ-CG (C) mixtures, and an individual WPI solution (D). Scale bar = 100 μm.

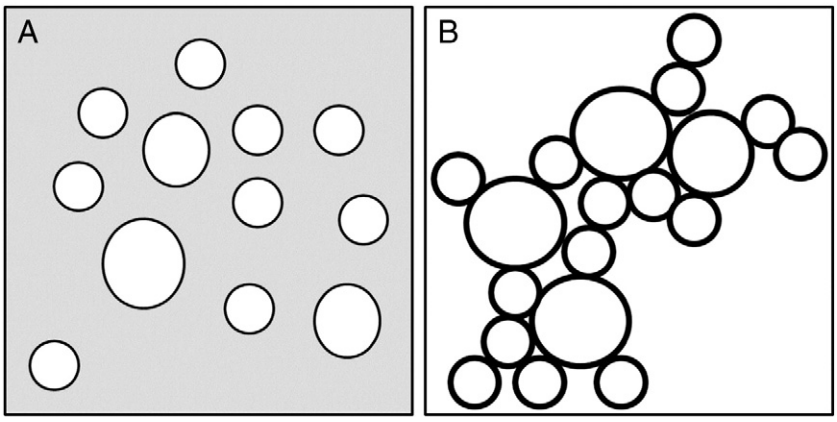

Fig. 10. Schematic of an emulsion-filled protein gel (A) and a protein stabilized-emulsion gel (B).

which reduced the flexibility of the oil–water interface causing the Du Nüoy ring to slip through it. As a result, reliable measurements could not be made after 45 min.

3.4. Rheology of WPI and WPI–carrageenan stabilized emulsions

Based on the surface activity of WPI and WPI–CG systems and their ability to reduce interfacial tension, emulsions were prepared at a 1:1 oil:water ratio, and then followed by rheological measurements over time, frequency and strain in a similar capacity as for the biopolymer solutions without oil. Fig. 6 shows changes to the viscoelastic moduli as a function of time/pH for all systems. The individual WPI stabilized emulsion formed a gel where the G′ became greater than G″ at a pH near 7.00 and then increased to a plateau upon over time/acidification as indicative of a gel network (Fig. 6A). Formed networks also showed greater elasticity than that of a non-emulsified system were G′ values were ~12.9 Pa (Fig. 6A) and ~0.2 Pa (Fig. 2A), respectively after 90 min.

n the case of the WPI–CG mixtures, the gel point (i.e., crossover point where G′ > G″) was found to occur at pHs ~6.0–6.5 (Fig. 6B–D). Moduli both increased gradually until ~pH 5.5, in which an inflection point was seen, followed by an even steeper rise in G′ and G″. This inflection point seemed to correspond to where complexation of WPI and CG molecules occurs. Moduli increased further until reaching a plateau. After 90 min, G′ values were ~452.9, 305.8 and 103.5 Pa for WPI–κ-CG, WPI–ι-CG and WPI–λ-CG mixtures, respectively (Fig. 6B–D). In all cases viscoelastic moduli were slightly higher in the emulsion gels than the systems without oil.

In a recent study by Santipanichwong and Suphantharika (2009), β-glucans were used to stabilize egg yolk emulsions. They reported that the addition of β-glucans enhanced the storage modulus of their emulsions and speculated the possibility for the β-glucans to enable a three dimensional network to form with the emulsified egg yolk emulsion (Santipanichwong & Suphantharika, 2009). Furthermore, differences in the modulus were found due to different β-glucan sources whereby all emulsions which were formed with β-glucans were found to be weak-gels under frequency sweep analysis (Santipanichwong & Suphantharika, 2009).

In the present study, viscoelastic moduli as a function of frequency for all systems showed gel-like behavior congruent with the time sweep experiments (Fig. 7). All moduli were also higher in magnitude than seen for the individual biopolymer solutions (no oil) (Figs. 3 and 7) indicating that a stronger network is being formed. Based on the strain sweep data, structure breakdown was more gradual as strain was increased, whereas the WPI–κ-CG (Fig. 8B) showed a strong break at ~17.77% strain reflective of its stiff network. Both WPI–ι-CG and WPI–λ-CG emulsion based systems also showed a strong break at ~9.33 and ~2.60% strains, respectively (Fig. 8C,D). The less amount of strain needed to induce structure breakdown suggests a slightly weaker network being formed.

3.5. Emulsion droplet sizes of WPI and WPI–CG emulsions

Emulsions were prepared, covered with a coverslip and left on a microscopy slide to acidify for 90 min before being imaged to observe the morphology of the gels at pH ~4.0–4.3. Images for WPI–κ-CG, WPI–ι-CG and WPI–λ-CG mixtures and for WPI alone are given in Fig. 9A, B, C and D, respectively. Mean droplet diameters within the WPI stabilized emulsion was found to be 37.88 ± 0.46 μm based on averaging the diameter of 50 droplets per slide for three slides. In contrast, mean droplet sizes for WPI–κ-CG, WPI–ι-CG and WPI–λ-CG stabilized emulsions were 32.95 ± 0.31 μm, 31.30 ± 0.23 μm and 32.41 ± 0.24 μm, respectively. The presence of CG decreased the average droplet size of these emulsions from ~38 to ~32 μm. Due to the incompressibility of the droplets, larger droplets would exert a larger frictional force marked by a larger storage modulus under rheology. Since the strength of these emulsions, observed *via* their storage modulus (G′), may be ranked as WPI–κ-CG > WPI–ι-CG > WPI–λ-CG > WPI control, droplet size seem to have little to no bearing on the strength of these gels. Therefore, it is the WPI–CG interactions and the network that they form which would explain the elasticity of these gels. In a review by Dickinson (2012), protein-stabilized emulsion gels were separated into two types: 1) an emulsion-filled protein gel and 2) a protein-stabilized emulsion gel (Fig. 10). In an emulsion-filled protein gel, oil droplets are embedded within a continuous gelled network (Fig. 10A) (Dickinson, 2012). The presence of oil droplets within this network serves to weaken the overall gel structure whereby the magnitude of G′ is smaller for the emulsion gel compared to the biopolymer gel (Dickinson, 2012). In a protein-stabilized emulsion gel, the proteins coat the oil droplets, followed by their gelation into a thick viscoelastic film on the droplet surface and flocculation, to eventually form a continuous gel network (Fig. 10B) (Dickinson, 2012). Typically, emulsion gels exhibit a greater G′ than biopolymer gels without oil. In the present study, emulsion gels are proposed to be formed. As the mixture is acidified from pH 7.00, proteins become reduced in charge to allow for greater interactions while at the interface. Upon reaching $pH_{\phi 1}$, complexation with the CG molecules *via* electrostatic attraction strengthens the viscoelastic film formed at the interface. This is followed by flocculation between droplets until an electrostatic-stabilized gel network is formed within the continuous phase at the evaluated conditions.

4. Conclusions

In the present work, all WPI–CG mixtures, regardless of the CG-type were able to form electrostatically coupled gel networks, however the network strength depended significantly on the CG-type present. Coupled networks were much stronger in the presence of κ-CG and ι-CG, than λ-CG, since the latter experienced far greater electrostatic

repulsion between chains than the other types. In the presence of oil, coacervation by CG with WPI at the interface affected the interfacial tension and enhanced emulsion stability. The effectiveness of CG influencing the rheology and emulsifying properties of WPI seems to be related to the linear charge density of the CG and possibly its conformation in solution. For instance, both κ-CG and ι-CG formed stronger electrostatic coupled networks with WPI, whereas because of the high number of sulfate groups on λ-CG structure formation was hindered from the large repulsive forces between polysaccharide chains ultimately leading to weaker networks than the other CG types. The interactions between WPI and CG and their functionality continue to be of interest to researchers. As further information is reported on these WPI–CG systems, this will aid manufacturers in knowing how to incorporate these mixtures in applications found in foods and cosmetics.

Nomenclature

ANOVA	analysis of variance
β	correction factor used to calculate the interfacial tension
CG	carrageenan
F_{max}	maximum force
γ	interfacial tension
G′	storage modulus
G″	loss modulus
GDL	glucono-δ-lactone
Hz	Hertz
mN/m	milli-Newton per meter
OD	optical density
Pa	Pascal
pH_c	pH associated with the formation of soluble complexes
$pH_{\phi 1}$	pH associated with the formation of insoluble complexes
$pH_{\phi 2}$	pH associated with the dissociation of complexes
pH_{opt}	pH associated with the maximum optical density
pI	pH associated with the isoelectric point
R	radius
rpm	revolutions per minute
μm	microns
WPI	whey protein isolate
w/w	weight per weight

Acknowledgments

Financial support for this research was provided by the National Science and Engineering Research Council of Canada (341731-2008) and the Canadian Dairy Commission (through scholarship support for RL).

References

Alizadeh-Pasdar, N., Nakai, S., & Li-Chan, E. C. Y. (2002). Principal component similarity analysis of Raman spectra to study the effects of pH, heating, and kappa-carrageenan on whey protein structure. *Journal of Agricultural and Food Chemistry*, *50*, 6042–6052.

Association of Official Analytical Chemists [AOAC] (2003). *Official method of analysis* (17th ed.). Washington DC USA: Association of Official Analytical Chemists.

Boral, S., & Bohidar, H. B. (2010). Effect of ionic strength on surface-selective patch binding-induced phase separation and coacervation in similarly charged gelatin–agar molecular systems. *Journal of Physical Chemistry B*, *37*, 12027–12035.

Britten, M., & Giroux, H. J. (1991). Emulsifying properties of whey-protein and casein composite blends. *Journal of Dairy Science*, *74*, 3318–3325.

Campo, V. L., Kawano, D. F., de Silva, D. B., & Carvalho, I. (2009). Carrageenans: Biological properties, chemical modifications and structural analysis — A review. *Carbohydrate Polymers*, *77*, 167–180.

Davis, J. P., & Foegeding, E. A. (2007). Comparisons of the foaming and interfacial properties of whey protein isolate and egg white proteins. *Colloids and surfaces. B, Biointerfaces*, *54*, 200–210.

de Kruif, C. G., Weinbreck, F., & de Vries, R. (2004). Complex coacervation of proteins and anionic polysaccharides. *Current Opinion in Colloid & Interface Science*, *9*, 340–349.

Dickinson, E. (2008). Interfacial structure and stability of food emulsions as affected by protein–polysaccharide interactions. *Soft Matter*, *4*, 932–942.

Dickinson, E. (2012). Emulsion gels: The structuring of soft solids with protein-stabilized oil droplets. *Food Hydrocolloids*, *28*, 224–241.

Dubin, P. L., Gao, J., & Mattison, K. (1994). Protein-purification by selective phase-separation with polyelectrolytes. *Separation and Purification Methods*, *23*, 1–16.

Elofsson, C., Dejmek, P., Paulsson, M., & Burling, H. (1997). Characterization of a cold-gelling whey protein concentrate. *International Dairy Journal*, *7*, 601–608.

Grasdalen, H., & Smidsrød, O. (1981). Iodide-specific formation of kappa-carrageenan single helices — I 127 NMR spectroscopic evidence for selective site binding of iodide anions in the ordered conformation. *Macromolecules*, *14*, 1842–1845.

Gulzar, M., Lechevalier, V., Bouhallab, S., & Croguennec, T. (2012). The physicochemical parameters during dry heating strongly influence the gelling properties of whey proteins. *Journal of Food Engineering*, *112*, 296–303.

Harrington, J. C., Foegeding, E. A., Mulvihill, D. M., & Morris, E. R. (2009). Segregative interactions and competitive binding of Ca^{2+} in gelling mixtures of whey protein isolate with Na^{+} kappa-carrageenan. *Food Hydrocolloids*, *23*, 468–489.

Hu, M., McClements, D. J., & Decker, E. A. (2004). Impact of chelators on the oxidative stability of whey protein isolate-stabilized oil-in-water emulsions containing omega-3 fatty acids. *Food Chemistry*, *88*, 57–62.

Hu, Y., Wang, H., Wang, J., Wang, S., Wang, L., Yang, Y., et al. (2010). Supramolecular hydrogels inspired by collagen for tissue engineering. *Organic & Biomolecular Chemistry*, *8*, 3267–3271.

Knutsen, S. H., Myladobodski, D. E., Larsen, B., & Usov, A. I. (1994). A modified system of nomenclature for red algal galactans. *Botanica Marina*, *37*, 163–169.

Koupantsis, T., Pavlidou, E., & Paraskevopoulou, A. (2014). Flavor encapsulation in milk proteins — CMC coacervate-type complexes. *Food Hydrocolloids*, *37*, 134–142.

Li, Y., & McClements, D. J. (2011). Controlling lipid digestion by encapsulation of protein-stabilized lipid droplets within alginate–chitosan complex coacervates. *Food Hydrocolloids*, *25*, 1025–1033.

McClements, D. J. (2005). *Food emulsions: Principles, practice and techniques* (2nd ed.). Boca Raton, FL USA: CRC Press Taylor & Francis Group.

Nakagawa, K., Iwamoto, S., Nakajima, M., Shono, A., & Satoh, K. (2004). Microchannel emulsification using gelatin and surfactant-free coacervate microencapsulation. *Journal of Colloid and Interface Science*, *278*, 198–205.

Parris, N., & Baginski, M. A. (1991). A rapid method for the determination of whey-protein denaturation. *Journal of Dairy Science*, *74*, 58–64.

Patino, J. M. R., Nino, M. R. R., & Sanchez, C. C. (1999). Dynamic interfacial rheology as a tool for the characterization of whey protein isolates gelation at the oil–water interface. *Journal of Agricultural and Food Chemistry*, *47*, 3640–3648.

Piculell, L., Nilsson, S., & Muhrbeck, P. (1992). Effects of small amounts of kappa-carrageenan on the rheology of aqueous iota-carrageenan. *Carbohydrate Polymers*, *18*, 199–208.

Rees, D. A., Scott, W. E., & Williamson, F. B. (1970). Correlation of optical activity with polysaccharide conformation. *Nature*, *227*, 390–392.

Reiffers-Magnani, C. K., Cuq, J. L., & Watzke, H. J. (2000). Depletion flocculation and thermodynamic incompatibility in whey protein stabilized O/W emulsions. *Food Hydrocolloids*, *14*, 521–530.

Rinaudo, M. (2006). Non-covalent interactions in polysaccharide systems. *Macromolecular Bioscience*, *6*, 590–610.

Rochas, C., & Landry, S. (1987). Molecular organization of kappa carrageenan in aqueous solution. *Carbohydrate Polymers*, *7*, 435–447.

Rochas, C., Rinaudo, M., & Vincendon, M. (1980). Structural and conformational investigation of carrageenans. *Biopolymers*, *19*, 2165–2175.

Santipanichwong, R., & Suphantharika, M. (2009). Influence of different β-glucans on the physical and rheological properties of egg yolk stabilized oil-in-water emulsions. *Food Hydocolloids*, *23*, 1279–1287.

Schmidt, I., Cousin, F., Huchon, C., Boue, F., & Axelos, M. A. V. (2009). Spatial structure and composition of polysaccharide–protein complexes from small angle neutron scattering. *Biomacromolecules*, *10*, 1346–1357.

Singh, S. S., Aswal, V. K., & Bohidar, H. B. (2007). Structural studies of agar–gelatin complex coacervates by small angle neutron scattering, rheology and differential scanning calorimetry. *International Journal of Biological Macromolecules*, *41*, 301–307.

Souza, H. K. S., Hilliou, L., Bastos, M., & Goncalves, M. P. (2011). Effect of molecular weight and chemical structure on thermal and rheological properties of gelling kappa/iota-hybrid carrageenan solutions. *Carbohydrate Polymers*, *85*, 429–438.

Stone, A. K., & Nickerson, M. T. (2012). Formation and functionality of whey protein isolate–(kappa-, iota-, and lambda-type) carrageenan electrostatic complexes. *Food Hydrocolloids*, *27*, 271–277.

Tang, Q. N., McCarthy, O. J., & Munro, P. A. (1994). Oscillatory rheological comparison of the gelling characteristics of egg-white, whey-protein concentrates, whey-protein isolate, and beta-lactoglobulin. *Journal of Agricultural and Food Chemistry*, *42*, 2126–2130.

Tavares, C., Monteiro, S. R., Moreno, N., & Lopes da Silva, J. A. (2005). Does the branching degree of galactomannans influence their effect on whey protein gelation? *Colloids and Surfaces A: Physicochemical and Engineering Aspects*, *270–271*, 213–219.

Tcholakova, S., Denkov, N. D., Ivanov, I. B., & Campbell, B. (2006). Coalescence stability of emulsions containing globular milk proteins. *Advances in Colloid and Interface Science*, *123*, 259–293.

Thanh, T. T. T., Yuguchi, Y., Mimura, M., Yasunaga, H., Takano, R., Urakawa, H., et al. (2002). Molecular characteristics and gelling properties of the carrageenan family, 1 — Preparation of novel carrageenans and their dilute solution properties. *Macromolecular Chemistry and Physics*, *203*, 15–23.

Trius, A., Sebranek, J. G., & Lanier, T. (1996). Carrageenans and their use in meat products. *Critical Reviews in Food Science and Nutrition*, *36*, 69–85.

Turgeon, S. L., Schmitt, C., & Sanchez, C. (2007). Protein–polysaccharide complexes and coacervates. *Current Opinion in Colloid & Interface Science*, *12*, 166–178.

van de Velde, F., Knutsen, S. H., Usov, A. I., Rollema, H. S., & Cerezo, A. S. (2002). ^{1}H and ^{13}C high resolution NMR spectroscopy of carrageenans: Application in research in industry. *Trends in Food Science & Technology*, *13*, 73–92.

Weinbreck, F., de Vries, R., Schrooyen, P., & de Kruif, C. G. (2003). Complex coacervation of whey proteins and gum arabic. *Biomacromolecules*, *4*, 293–303.
Weinbreck, F., Nieuwenhuijse, H., Robjijn, G. W., & de Kruif, C. G. (2004). Complexation of whey proteins with carrageenan. *Journal of Agricultural and Food Chemistry*, *52*, 3550–3555.
Yang, X., & Foegeding, E. A. (2011). The stability and physical properties of egg white and whey protein foams explained based on microstructure and interfacial properties. *Food Hydrocolloids*, *25*, 1687–1701.
Yuan, Y., Wang, Z. L., Yang, X. Q., & Yin, S. W. (2014). Associative interactions between chitosan and soy protein fractions: Effects of pH, mixing ratio, heat treatment and ionic strength. *Food Research International*, *55*, 207–214.